

MrGCN: Mirror Graph Convolution Network for Relation Extraction with Long-Term Dependencies

I-Hung Hsu^{1*}, Xiao Guo^{1*}, Wael AbdAlmageed¹, Premkumar Natarajan¹, Nanyun Peng^{1,2}

¹ Information Sciences Institute, University of Southern California

² Computer Science Department, University of California, Los Angeles

{xiaoguo, ihunghsu, wamageed, pnataraj} @isi.edu;
violetpeng@cs.ucla.edu

Abstract

The ability to capture complex linguistic structures and long-term dependencies among words in the passage is essential for relation extraction (RE) tasks. Graph neural networks (GNNs), one of the means to encode dependency graphs, have been shown to be effective in prior works. However, relatively little attention has been paid to *receptive fields* of GNNs, which can be crucial for tasks with extremely long text that requires discourse understanding. In this work, we leverage the idea of *graph pooling* and propose the Mirror Graph Convolution Network, a GNN model with a pooling-unpooling structure tailored to RE tasks. The pooling branch reduces the graph size and enables the GNN to obtain larger *receptive fields* within fewer layers; the unpooling branch restores the pooled graph to its original resolution for token-level RE tasks. Experiments on two discourse-level relation extraction datasets demonstrate the effectiveness of our method, showing significant improvements over prior methods especially when modeling long-term dependencies is necessary. Moreover, we propose Clause Matching (CM), a novel graph pooling method that merges nodes based on dependency relations in graph. CM can largely reduce the graph size while retaining the main semantics of the input text.

1 Introduction

Relation extraction (RE), the task to extract the relation between entities in the text, is an important intermediate step for downstream tasks in natural language processing (NLP). While earlier works in RE focus on binary relations (relations that only involve two entities) within a single sentence (Miwa and Bansal, 2016), recent works place more emphasis on identifying the relation between entities that appear in different sentences or require a large context to disambiguate (Gupta et al., 2019; Aki-moto et al., 2019). For example, Peng et al. (2017)

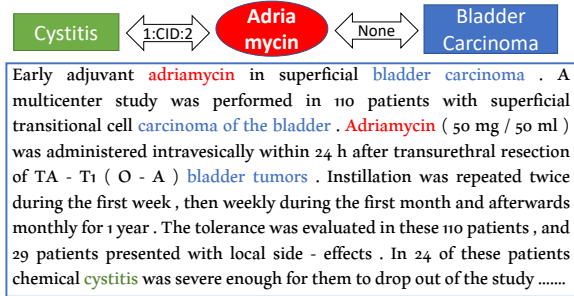


Figure 1: An example of document-level relations from the CDR dataset. The oval represents chemical **Adriamycin**, and rectangles represent two diseases: **Bladder Carcinoma** and **Cystitis**. Reading the whole passage over six sentences is essential to the understanding about the relation between **Adriamycin** and **Cystitis**.

study RE for entity mentions spanning multiple sentences, and Li et al. (2016a) provide a chemical-disease reactions (CDR) dataset that annotates binary relations between entities at *document-level*.

While these settings are practical, they bring special challenges to NLP models. Most notably, the models need to capture *long-term dependencies* between words to catch relations between entities spanning several sentences. For example, in Fig. 1, the relation between **Cystitis** and **Adrimycin** can only be understood by considering the whole paragraph. In order to learn such long-term dependency, prior works incorporate dependency trees to capture syntactic clues in the non-local manner (Miwa and Bansal, 2016; Zhang et al., 2018), where graph neural networks (GNNs) has been widely applied (Peng et al., 2017; Sahu et al., 2019). However, the *receptive fields* (Luo et al., 2016) of GNNs, which measure the information range that a node in a graph can access, are less discussed. In theory, a large *receptive field* of GNNs is essential for learning representations that capture extremely *long-term dependencies*.

Inspired by the recent development of *graph pooling* with a pooling-unpooling structure in GNNs for graph representation learning (Gao and

* The authors contribute equally, random order.

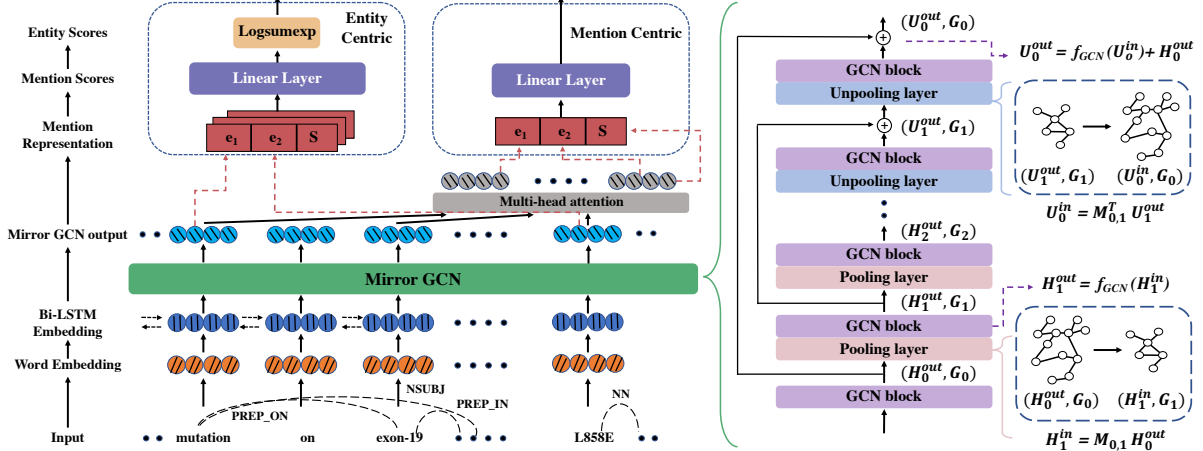


Figure 2: Mirror Graph Convolutional Network (MrGCN) for RE tasks. **Left:** The overall architecture: the **word embeddings** from the input text are fed to the Bi-LSTM layer and **Mirror GCN** to learn representations for each token. The **output features** are then used for the entity-centric or mention-centric RE. **Right:** Details of **Mirror GCN**. Input graph embeddings flow through a GCN block, several pooling layers and unpooling layers to aggregate information with different scales. G_i represents hypergraphs at the i -th level. H_i^{in} and U_i^{in} denote the converted embeddings after the pooling and unpooling layers in i -th hypergraph using the matching matrix $M_{l,l+1}$ and the residual connections. H_i^{out} and U_i^{out} are the refined representations after GCN blocks.

Ji, 2019; Yu et al., 2019), we adapt such a paradigm and propose the Mirror Graph Convolutional Network (MrGCN), which has a symmetric structure with the pooling-unpooling mechanism (as depicted in Fig. 2). In the pooling branch, we use *graph pooling* to convert the input document graph to a series of more compact hypergraphs by merging structurally similar or related nodes into *supernodes*, which serve as their information union. The graph convolution operation on the hypergraphs thus aggregates a larger neighborhood of features, increasing the size of the *receptive field* for each node. Then, the unpooling layers are used to restore global information in hypergraphs back to the original graph such that token-level RE can be performed. With such a pooling-unpooling mechanism, each graph node obtains richer features.

We explore two graph pooling strategies: Hybrid Matching (HM) and Clause Matching (CM). Hybrid Matching (Liang et al., 2018) matches nodes based on the structural similarity, and has been shown to be effective in learning graph embeddings. However, HM ignores information of edge types. Thus, we propose Clause Matching which leverages the type of dependent arcs to merge nodes. Comparing to HM, which is a general graph pooling algorithm that merges nodes by considering the overall graph structure, CM is designed from the linguistic perspective in that CM places emphasis on dependent relations. Despite the differences, MrGCN with either pooling method achieves sub-

stantial improvements over baselines on the two RE datasets.

Our contributions are: (1) We propose MrGCN to tackle discourse-level RE tasks. MrGCN is compatible with two different graph pooling methods and achieves substantial improvements over baselines on two datasets. (2) We introduce a new graph pooling method for RE tasks – Clause Matching, which merges tokens based on their dependency relations. Clause Matching method can largely reduce the graph size while keeping basic semantic structure of the input. (3) We conduct a novel analysis regarding *entity distance* in graph, and carry out comprehensive studies to demonstrate MrGCN’s superb ability on handling relations among entities with long distances.

2 Background

Task Definition. In the paper, we study two RE tasks, mention-centric RE and entity-centric RE. Mention-centric RE predicts relation R of given entity mentions, e_1, \dots, e_n , in the context T . Entity-centric RE identifies the relation R among E_1, \dots, E_m , where E_i indicates an entity and each entity can have multiple entity mentions in T . For example, *adriamycin* is mentioned twice in Fig. 1.

Document Graph. Document graph (Quirk and Poon, 2016) represents intra- and inter-sentential dependencies in texts. It consists of nodes representing words and edges representing various dependencies among words. Typically, two words

can be linked if they (1) are adjacent, (2) have dependency arcs, or (3) share discourse relations, such as coreference or being roots of sequential sentences. We use document graphs to represent input texts and apply our model to them for leveraging syntactic and discourse clues in the input.

3 Proposed Method

Our proposed MrGCN, as depicted in Fig. 2, is a symmetric architecture with a pooling-unpooling mechanism. The input text is first encoded into contextualized embedding via word embedding and BiLSTM layers. Then such contextualized embeddings are fed into MrGCN to learn representations for each token. Depending on the RE task, the learned token representations are used differently for the final prediction. Specifically, the pooling layer deterministically converts a graph into a more compact *hypergraph* using *matching matrices* generated by graph pooling methods (Sec. 3.1). After that, GCN blocks are employed to update the graph embeddings for each hypergraph (Sec. 3.2). The unpooling layer performs a reverse operation to the pooling layer, restoring finer-grain graphs from the hypergraphs to the original graph (Sec. 3.3). Lastly, task-specific RE models are built using the learned representations (Sec. 3.4). The architecture is trained in an end-to-end fashion.

3.1 Graph Pooling

Graph pooling iteratively coarsens graph G into a smaller but structurally similar graph G' . It usually first discovers nodes that can be grouped (Ying et al., 2018; Lee et al., 2019). Then, nodes that are matched together will be merged into a *supernode*. We introduce *Hybrid Matching* (HM) and our proposed *Clause Matching* (CM) in this section.

Hybrid Matching. Hybrid Matching (Liang et al., 2018) is shown to be effective for learning large-scale graph embeddings. It performs node matching based on the connectivity between nodes and consists of *structural equivalence matching* (SEM) and *normalized heavy edge matching* (NHEM).

SEM merges two nodes that share the exact same neighbor. In the Fig. 3 example, node n_0 and n_2 are considered as structural equivalence, since they share the exact same neighbor node n_1 .

NHEM uses the adjacency matrix A to perform matching. Each node will be matched with its neighbor that has the largest *normalized edge weight* (NEW) and supernodes cannot be merged

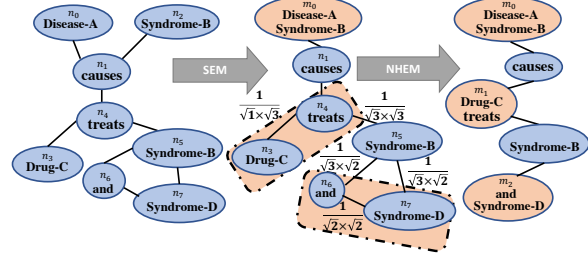


Figure 3: The illustration of Hybrid Matching (HM) for the instance “Disease-A causes Syndrome-B. Drug-C treats Syndrome-B and Syndrome-D” with target entities “Disease-A”, “Drug-C” and “Syndrome-D”. HM consists of two steps: SEM and NHEM. After performing HM, distances from “Drug-C” to “Disease-A”, and from “Drug-C” to “Syndrome-D” decrease by 1.

again. The *normalized edge weight*, $N(u, v)$, for each edge in the graph is defined as:

$$N(u, v) = \frac{A_{uv}}{\sqrt{D(u) \times D(v)}}, \quad (1)$$

where $D(u)$ is the degree of node u . The adjacency matrix A of the original input document graph (i.e, A^0) has cell value A_{uv}^0 being either 1 or 0, indicating if a connection from node u to v exists or not. As for adjacency matrix for pooled graph, it can be calculated based on its parent graph (see Eq. 3).

In NHEM, we visit nodes by ascending order according to the node degree following Liang et al. (2018), and we illustrate the process in Fig. 3. After computing NEW of the graph, we first visit node n_3 (degree equals 1), and merge it with its only neighbor n_4 into the supernode m_1 . Then, we visit node n_6 and merge it with n_7 that has the largest NEW with n_6 . Since supernodes cannot be merged again in each round of HM, n_1 and n_5 remain. After HM, distances among targeted entities decrease.

Clause Matching. The edge attribute is important to group nodes in the document graphs. For example, “a red apple” can be split into three nodes in the document graph, although they are essentially one noun phrase. The dependency tree shows that “a” is the determiner (det) of “apple”, and “red” is an adjectival modifier (amod). Such edge information should be considered in the pooling operation, but has been ignored by many general graph pooling method like HM. Therefore, we propose Clause Matching (CM), which merges tokens based on the dependency relation between them.

Specifically, following De Marneffe et al., we first classify dependency relations into two categories – *core arguments* and *others*. *Core arguments* link predicates with their core dependents,

Algorithm 1 Clause Matching

Require: $G = (V, E)$, $E \subseteq \{e = (v_i, v_j) | (v_i, v_j) \in V^2\}$.
Require: Edge type function f_T : $f_T(e)$ = the edge type of e .
Require: Mergeable edge type set T .

- 1: Sort V by the number of neighbors in ascending order.
- 2: $C = \emptyset$ # The set collects nodes that have merged others.
- 3: **for** $v_i \in V$ **do**
- 4: **if** $v_i \notin C$ **then**
- 5: **for** $v_j \in \{v_j | v_j \in V; (v_j, v_i) \in E\}$ **do**
- 6: **if** $f_T(e = (v_j, v_i)) \in S$ **then**
- 7: $V = V \setminus \{v_i\}$ # Merge v_i to v_j
- 8: **for** $v_k \in \{v_k | v_k \in V; (v_k, v_i) \in E\}$ **do**
- 9: # Move edges in v_i to v_j
- 10: $E = E \setminus \{(v_k, v_i)\}$
- 11: $E = E \cup \{(v_k, v_j)\}$
- 12: $C = C \cup \{v_j\}$
- 13: **break**
- 14: **return** Pooled graph $G = (V, E)$

as a clause should at least consist of a predicate with its core dependents¹. CM merges tokens that are connected by dependency relations in *others* categories². Since we do not merge nodes linked with *core arguments*, the basis of a clause will be retained. As a result, CM simplifies the graph and maintains the core components of a clause.

The details of CM is in Alg. 1³. CM share similarities with HM: i). we visit nodes by ascending order according to the node degree (line 1); ii). supernodes cannot be merged again in each round of CM (line 4). Being different from HM, we decide whether the visited node can be merged with its dependent head based on the edge type (line 6-7)⁴.

In Fig. 4, we show an example of CM and more visualizations are in the appendix (Fig. 7). We first visit $n_0, n_2, n_4, \dots, n_5$ in order, based on node degree. When visiting n_0 , CM matches n_0 with its dependent head n_1 because the dependent arc between them belongs to *others* types. Similarly, n_2 is merged with n_3 and n_4 is matched with n_5 , forming m_1 and m_2 , respectively. However, m_2 cannot be further combined with m_1 because m_2 is already a supernode in the current round of CM. Moreover, m_0 cannot be merged with m_1 even if we perform CM again because the dependency arcs “nsubj:pass” belongs to *core arguments*.

Pooling Operation. Each matching process generates a coarsened hypergraph. Performing match-

¹Following the definition in Universal Dependency: www.universaldependencies.org/u/overview/simple-syntax.html.

²E.g., “det” and “amod” are not core arguments but others.

³The set T is defined as $\{\text{all dependency edges}\} \setminus \{\text{“nsubj”, “nsubj:pass”, “dobj”, “iobj”, “csubj”, “csubj:pass”, “ccomp”, “xcomp”}\}$.

⁴When moving edges from children nodes to supernodes, we do not include self-loop causing by merging.

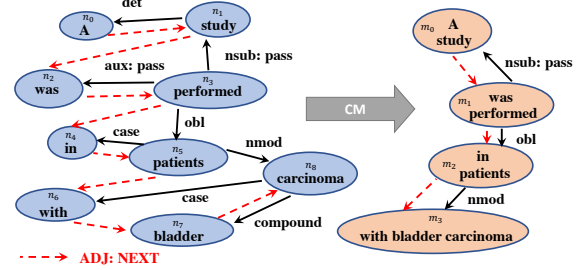


Figure 4: The visualization of Clause Matching (CM), given input “A study was performed in patients with bladder carcinoma”. “ADJ:NEXT” indicates the adjacency edges. After executing CM once, the graph size reduces largely yet still maintain the core structure of the original sentence.

ing L times produces L hypergraphs with increasing coarsening levels, denoted as G_0, G_1, \dots, G_L , where G_0 is the initial graph. We use *matching matrix* $M_{l-1,l}$ to mathematically represent the merging process from level $l-1$ to level l . $M_{l-1,l} \in \mathbb{R}^{n \times m}$ converts $G_{l-1} \in \mathbb{R}^{n \times n}$ to $G_l \in \mathbb{R}^{m \times m}$ with $n \geq m$. Each cell m_{ij} in $M_{l-1,l}$ is:

$$m_{ij} = \begin{cases} 1, & \text{if node } i \text{ is matched into supernode } j. \\ 0, & \text{otherwise.} \end{cases} \quad (2)$$

With $M_{l-1,l}$ constructed, we can compute the adjacency matrix of level l , A^l , based on A^{l-1} ⁵:

$$A^l = M_{l-1,l}^T A^{l-1} M_{l-1,l}, \quad (3)$$

and perform representation transformation to get the *initial* node embeddings for the next level:

$$H_l^{in} = M_{l-1,l} H_{l-1}^{out} \quad (4)$$

where H_{l-1}^{out} and H_l^{in} represent the output embedding of G_{l-1} and the input embedding of G_l .

3.2 Graph Convolutional Network

Given the hypergraphs that we have generated through graph pooling, graph convolution networks (GCN) (Kipf and Welling, 2016) is executed to update node embeddings on the hypergraphs. We stack S layers ($S \in \mathbb{Z}^+$) of GCN for a GCN block, and we do not adopt complex techniques, such as incorporating directionality or edge-wise gates (Bastings et al., 2017; Marcheggiani and Titov, 2017) for simplicity.

With the adjacency matrix A we introduced before, the operation of the GCN block is:

$$h_i^l = \text{RELU} \left(\sum_{j=1}^N A_{ij}^l W^l h_j^{l-1} + b^l \right), \quad (5)$$

⁵The same as in Hybrid Matching. More detail can be seen in the appendix (Fig 6).

where h_i^l is the representation of node i in the l -th graph, and W^l and b^l are the corresponding weight and bias term. We define the output embedding H_l^{out} of G_l as $H_l^{out} = f_{GCN}(H_l^{in})$, where f_{GCN} approximates the GCN block function.

3.3 Graph Unpooling

After several layers of graph pooling, MrGCN encodes information with enlarged receptive field into the coarsest-grain hypergraph. The unpooling branch then restores and refines the information to the original resolution for downstream tasks.

Specifically, the unpooling layers use the matching matrices from the pooling layers and perform reverse operations, including generating larger graphs and mapping the embeddings to unpooled graphs. Each unpooling layer is followed by a GCN block to finetune representations. We denote the unpooling operation on l th graph embedding as:

$$U_{l-1}^{in} = M_{l-1,l}^T U_l^{out}, \quad \widetilde{U}_{l-1}^{out} = f_{GCN}(U_{l-1}^{in}). \quad (6)$$

Additionally, we add the residual connection to perform element-wise summation from corresponding embeddings in pooling branch as depicted in Fig. 2, i.e. $U_{l-1}^{out} = \widetilde{U}_{l-1}^{out} + H_{l-1}^{out}$. This operation not only combines information at different scales but also prevents the architecture from potential degradation with increasing layers (He et al., 2016).

3.4 Apply to Relation Extraction

The node embeddings obtained from MrGCN encoded comprehensive features for each token in the input text. We now introduce how to apply such features to mention-centric and entity-centric RE.

Mention-centric RE. We first add an multi-head self-attention layer to perform a final refinement for token representations. Embeddings of the tokens that are entity mentions are concatenated with the additional max-pooled sentence embedding, and then fed into linear layers for the final classification. Fig. 2 illustrates the whole process.

Entity-centric RE. In entity-centric RE, only relation labels for entities are available. Due to the coarse-grained learning signal, it is hard to evaluate the contribution of each mention pair. To accumulate all the information for each mention pair and produce per-relation score for the entity pair, we adopt the method from Verga et al. (2018); Jia et al. (2019) to use the LogSumExp to aggregate information from multiple mentions of the given entities:

$$score(E_1, E_2) = \log \sum_{e_1 \in E_1, e_2 \in E_2} \exp(g(e_1, e_2)), \quad (7)$$

where $score(E_1, E_2)$ is the final logit for entity pair (E_1, E_2) , and $g(e_1, e_2)$ is the score for the given mention tuple e_1 and e_2 ⁶.

4 Experiments

We conduct experiments on two RE datasets, the Cross-Sentence n -ary Dataset and the Chemical-Disease Reactions Dataset⁷.

4.1 Cross-Sentence n -ary Dataset

Data and Task Settings: The cross-sentence n -ary dataset (n -ary) (Peng et al., 2017) contains drug-gene-mutation ternary and drug-mutation binary relations annotated via distant supervision (Mintz et al., 2009). For this dataset, we investigate two experimental setups: (1) *Entity Anonymity*, which replaces target entities with dummy tokens to prevent the classifier from simply memorizing the entity names. It is a standard practice in distant supervision RE (Jia et al., 2019); (2) *Entity Identity*, where all tokens are exposed to the model.⁸

Implementation Details: The document graphs are provided in the original released n -ary dataset.⁹ We follow previous measurements – average accuracy of 5-fold cross-validation,¹⁰ and use GloVe vectors for word embeddings initialization.

Results on n -ary dataset: Table 1 shows the performance comparison on the n -ary dataset. We report results of our method with two pooling variations, i.e., MrGCN(CM) and MrGCN(HM), representing MrGCN with Clause Matching and with Hybird Matching, respectively. To fairly compare our method with baselines without BiLSTM, we also report the results from MrGCN ablating BiLSTM. We first compare our performance

⁶We try multi-head self-attention in entity-centric model, but it works worse than the model without attention. Our hypothesis is that the learning signal in entity-centric tasks are too weak to learn extra parameters in the attention, especially in the case where long context needs to be considered.

⁷Dataset statistics, best hyper-parameters (S layers of GCN in GCN block and level L of pooling times), and other implementation details are stated in the appendix A & B.

⁸Prior works are inconsistent w.r.t. this experimental detail. Specifically, Peng et al. (2017) conducted experiments under *Entity Anonymity* setup, while Song et al. (2018) and Guo et al. (2019) reported results under *Entity Identity* setup. For fair comparisons, we report results under both settings.

⁹www.github.com/VioletPeng/GraphLSTM_release

¹⁰Our data setup follows Song et al. (2018).

| Model | | Detection | | Classification | |
|-----------|-----------------|-------------|-------------|----------------|-------------|
| | | Ter. | Bin. | Ter. | Bin. |
| Anonymity | Graph LSTM | 80.7 | 76.7 | N/A | N/A |
| | AGGCN | 76.7 | 79.0 | 67.5 | 67.9 |
| | MrGCN(CM) | 83.3 | 81.5 | 77.4 | 76.0 |
| | w/o BiLSTM | 82.5 | 80.8 | 75.4 | 73.4 |
| | MrGCN(HM) | 83.6 | 81.4 | 78.3 | 76.5 |
| | w/o BiLSTM | 82.2 | 80.8 | 76.2 | 75.1 |
| | GS GLSTM | 83.2 | 83.6 | 71.7 | 71.7 |
| | GCN (Full Tree) | 84.8 | 83.6 | 77.5 | 74.3 |
| Identity | AGGCN | 87.0 | 85.6 | 79.7 | 77.4 |
| | MrGCN(CM) | 91.5 | 93.5 | 91.4 | 93.7 |
| | w/o BiLSTM | 91.4 | 93.9 | 90.8 | 93.6 |
| | MrGCN(HM) | 91.6 | 94.1 | <u>91.3</u> | 95.3 |
| | w/o BiLSTM | 91.5 | 94.0 | 90.8 | 94.7 |

Table 1: Results in average accuracy (%) of five-fold cross validation on the n -ary dataset for 4 sub-tasks. We compare MrGCN(CM) and MrGCN(HM), with Graph LSTM (Peng et al., 2017) and AGGCN (Guo et al., 2019) in Entity Anonymity, and with GS GLSTM (Song et al., 2018), GCN (Full Tree) (Zhang et al., 2018), and AGGCN under Entity Identity.

with prior works, GS GLSTM (Song et al., 2018), GCN (Full Tree) (Zhang et al., 2018)¹¹, and AGGCN (Guo et al., 2019), under Entity Identity setup. As the lower part of Table 1 shows, we outperform previous works by a large margin even without BiLSTM (at least 4.4% improvements in accuracy across all tasks). With the help of BiLSTM, our model can further improve the results.

In Entity Anonymity, we compare MrGCN with Graph LSTM (Peng et al., 2017) and AGGCN (Guo et al., 2019).¹² Results show that both of our methods surpass the previous best results by at least 2.4% accuracy. Again, the superiority of our method holds even on models without BiLSTM, which have at least 1.8% improvement over prior works. Although MrGCN(CM) shows some advantages in detection tasks, MrGCN(HM) works slightly better than MrGCN(CM) in general. We hypothesize the reason being the original document graphs in the n -ary dataset miss some unimportant dependency arcs, which prevent CM from merging nodes. However, HM takes all edges into consideration, hence, it can still efficiently merge nodes.

4.2 Chemical-Disease Reactions Dataset

Data: The chemical-disease reactions dataset (CDR) (Li et al., 2016a) was created from Comparative Toxicogenomics Database (CTD) (Davis

¹¹The result is adapted from Guo et al. (2019).

¹²The reported results of AGGCN in the upper of Table 1 are from our re-implementation by modifying their released code to make it match Entity Anonymity setup.

| Model | P | R | F1 |
|-----------------------------|-------------|-------------|-------------|
| Gu et al. (2017) | 55.7 | 68.1 | 61.3 |
| Verga et al. (2018) | 55.6 | 70.8 | 62.1 |
| Nguyen and Verspoor (2018) | 57.0 | 68.6 | 62.3 |
| Christopoulou et al. (2019) | 62.1 | 65.2 | 63.6 |
| MrGCN(CM) | 61.7 | 69.9 | 65.6 |
| MrGCN(HM) | 63.9 | 65.6 | 64.7 |
| Peng et al. (2016) | 62.1 | 64.2 | 63.1 |
| Li et al. (2016b) | 60.8 | 76.4 | 67.7 |
| Verga et al. (2018) + Data | 64.0 | 69.2 | 66.2 |

Table 2: Precision (P), recall (R), and F1 results on the test set in CDR. We compare MrGCN model with baseline models. Methods below the double line use additional training data.

et al., 2019), which only contains document-level labels between entities and do not contain mention annotation. CDR dataset is a subset of CTD supplemented with manual mention span labels, forming CDR an entity-centric document-level RE task.

Implementation Details: Unlike the n -ary dataset, no document graph is provided in the original CDR dataset, so we generate its document graphs similar to Sahu et al. (2019) using Stanford CoreNLP (Manning et al., 2014). We follow Christopoulou et al. (2019)¹³ to train the model in two steps. First, we train our model using standard training set and record the best number of epoch when the model reaches optimal on the validation set. Then, the model is re-trained using the union of the training and development data with the recorded number of epoch.

Results on CDR dataset: The result of MrGCN on CDR dataset is shown in Table 2. Some of the previous works include additional data in CTD dataset (Peng et al., 2016; Li et al., 2016b; Verga et al., 2018) as extra training data and achieved better results on the CDR dataset. However, we do not use such data, thus, we compare MrGCN with models that use only official data. As shown in Table 2, both our models outperform prior works by at least 1.1 F1 and MrGCN(CM) outperforms MrGCN(HM) on CDR dataset by 0.9 F1.

5 Analysis and Discussion

In this section, we investigate how MrGCN benefits from its components and verify the hypothesis that *Graph Pooling* is especially efficient for capturing long-term dependencies.

¹³We also follow them to use (1) GENIA Sentence Splitter for sentence splitting (2) GENIA Tagger (Tsuruoka et al., 2005) for tokenization (3) PubMed pre-trained word embeddings (Chiu et al., 2016).

| Model | n-ary | | | | CDR | |
|---------------------|--------------|-------------|----------------|-------------|--------------|--|
| | Detection | | Classification | | | |
| | Ter. | Bin. | Ter. | Bin. | | |
| MrGCN(CM) | 83.3* | 81.5 | 77.4** | 76.0 | 65.6* | |
| MrGCN(HM) | 83.6* | 81.4 | 78.3* | 76.5 | 64.7* | |
| MrGCN-pool | 82.2 | 81.2 | 76.8 | 76.2 | 62.7 | |
| MrGCN(CM)-RNN | 82.5 | 80.8* | 75.4* | 73.4* | 63.1* | |
| MrGCN(HM)-RNN | 82.2 | 80.8* | 76.2* | 75.1* | 61.9* | |
| MrGCN-pool-RNN | 82.0 | 80.1 | 73.8 | 70.0 | 60.2 | |
| MrGCN-pool-RNN-Att. | 77.4 | 79.1 | 70.3 | 71.2 | N/A | |

Table 3: Ablation studies. We report average accuracy for *n*-ary and F1 for CDR dataset. Ter. and Bin. stand for ternary and binary relation, respectively. No multi-head attention (Att.) component in models in the entity-centric dataset (e.g. CDR), so the setting in the last row is N/A. * and ** indicates the model outperforms its corresponding model without pooling with p-value < 0.01 and < 0.05 per McNemar’s test, respectively. **Bold** and *italic* indicate the best in each task and without RNN, respectively.

Noted that Entity Anonymity setup is more principled under the distant supervision setting, so in this section, the results on the *n*-ary dataset are obtained under the Entity Anonymity setup.

5.1 Ablation Studies

We present ablation studies in Table 3. For models *without RNN* (Rows 4-6), by comparing the models with and without pooling, we observe that graph pooling indeed significantly improved the performances on both datasets. Likewise, ablating pooling from full MrGCN models (Rows 1-3) leads to significant performances decrease, especially on the CDR dataset. Also, the benefits brought by the pooling mechanism is more significant on the CDR dataset and *n*-ary dataset’s ternary cases, where we anticipate longer distances between entities. BiLSTM (RNN) layers are useful for both datasets, and the attention mechanism is also efficient. Importantly, graph pooling is shown to be complimentary to these mechanisms as it brings performance gains on top of these sophisticated techniques.

5.2 Performance against Input Length

We follow Song et al. (2018) to conduct analysis about model performance against input length, which has been reported in Fig. 5a. In CDR dataset, the performance differences between models with and without pooling gradually increase when the input sentences grow longer, especially when the text length is over 375 tokens (while the difference is not significant when the input sentence is less than 250 words). In *n*-ary dataset, the performance gap between models with and without pooling is

significant when sentence length is between 75 to 100, yet the performances within shorter sentence length are similar. Such observations demonstrates that the pooling-unpooling mechanism helps cases with longer context.

Surprisingly, in CDR dataset, MrGCN suffers from a performance drop on instances with sentence length between 325 and 375, which we hypothesize is due to our model selection strategy. Specifically, we select the model according to the overall performance, hence, the final model can possibly be biased.¹⁴ Yet, another notable observation is that there is no significant performance drop for MrGCN without pooling on lengthier input. We hypothesize that sentence length is unnecessarily the best to measure long-term dependencies between entities. For instance, intuitively, although the inputs are long, the entities of interests are neighboring. Hence, we propose *entity distance* to study the model performance.

5.3 Performance against Entity Distance

We compute the *entity distance* in the document graph for each instance. For mention-centric RE, we calculate the minimum distance between mentions in the graph, denoted as *mention-pair distance*.¹⁵ Notably, in the ternary relation, the entity distance is the maximum value among three *mention-pair distance*, since such an upper-bound estimation reflects the largest effort to capture the required dependencies. Similarly, for entity-centric RE, we first calculate the *mention-pair distance* between each targeted mention pairs that belongs to entity-pairs of interests. Then, we take the maximum value over all *mention-pair distance*.

Fig. 5b shows the result of MrGCN against different entity distance. We can observe that the performance for all models degrade significantly in CDR when the entity distance increases. In *n*-ary dataset, unlike the Fig. 5a, the performances for model without pooling do not increase significantly as the entity distance grows. Such two tendencies indicate that *entity distance* may reflect long-term dependencies between entities more precisely. Also, with the help of graph pooling, MrGCN consistently outperforms MrGCN-pooling when *entity distance* is larger than 4 in CDR, 3 in *n*-ary, which supports the effectiveness of using graph pooling for capturing long-term dependencies.

¹⁴The hypothesis also explains the phenomenon in Fig. 5b

¹⁵If mentions contain multiple tokens, we calculate average distances between each token pairs in the mention-pair.

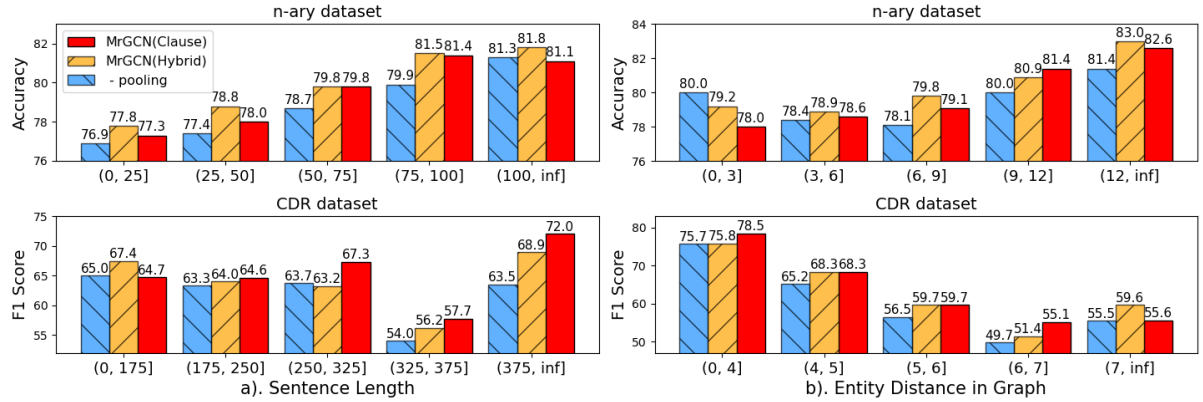


Figure 5: Performance against input length and entity distance in graph.

6 Related work

Relation Extraction Beyond Single Sentence. Peng et al. (2017) extend traditional RE to discerning the relation between n ($n \geq 2$) entities in the cross sentence scenario, and use two graph LSTM to encode the full document graph. However, information may be lost by dividing the whole graph into two halves. Song et al. (2018) apply a GNN on the entire graph, yet the receptive field scale in the method merely allows each node to see information within 5-hop distances. Soft pruning strategy from (Guo et al., 2019) forces each node to connect all other nodes using virtual edges. This ignores the original structural information of the input graph. MrGCN not only enlarges the receptive field scale but also maintains the graph structure information.

Another thread of related works is the entity-centric RE on document-level. Sahu et al. (2019) build a labelled edge GCN model to use non-local dependencies presented in document graph to perform RE prediction. Jia et al. (2019) propose a multi-scale representation learning approach, where final entities representation is merged from many smaller contexts embedding. Christopoulou et al. (2019) use rules to build edge representation from nodes and perform prediction based on edges. Our method learns better representations, thus can be migrated to improve both their works.

Graph Pooling in NLP. Graph pooling is a classic idea to learn representation associated with graph and can largely preserve the graph structure (Duvenaud et al.; Chen et al., 2018a). There are a few works that leverage such idea for NLP tasks. (Gao et al., 2019) adopts graph pooling to aggregate all local features for global text representation, via an “asymmetric” architecture without the unpooling operation, which differs from our work. Nguyen and Grishman (2018) has also explored the idea of

pooling with GCN, but their pooling is conducted on layer-wise output features instead of input graph. To the best of our knowledge, we are the first to apply idea of graph pooling on RE.

Pooling-unpooling Mechanism. The pooling-unpooling mechanism is widely-used for pixel-wise representation learning (Badrinarayanan et al., 2017; Chen et al., 2018b), which use downsampling and upsampling operation to aggregate information from different resolution. The flagship work of such paradigm is U-Net (Ronneberger et al., 2015), which demonstrates the effectiveness in the image segmentation. It is worth mentioning that Gao and Ji (2019) adopts such paradigm for graph node and graph classification task, and shares with our work similarity from the architectural perspective. However, the main contribution of them is the specially-designed pooling and unpooling operations. In contrast, our work focuses the effectiveness of such symmetric architecture in RE with long-term dependencies and a domain-specific designed pooling method.

7 Conclusion and Future Work

In this work, we explore the effectiveness of applying graph pooling-unpooling mechanism for representation learning in RE tasks. Such paradigm helps the model learn larger receptive fields for graph nodes and achieve better performances in tasks that requires learning long-term dependencies. Besides, we introduce a new graph pooling strategy that is tailored for NLP tasks.

For the future work, we plan to explore the possibility of applying the pooling-unpooling mechanism to other document-level NLP tasks. We also plan to propose differentiable, feature-selection free pooling methods that consider edge types to better serve the NLP community.

References

Kosuke Akimoto, Takuya Hiraoka, Kunihiko Sadamasa, and Mathias Niepert. 2019. [Cross-sentence n-ary relation extraction using lower-arity universal schemas](#). In *Proceedings of the 2019 Conference on Empirical Methods in Natural Language Processing and the 9th International Joint Conference on Natural Language Processing (EMNLP-IJCNLP)*, pages 6224–6230, Hong Kong, China. Association for Computational Linguistics.

Vijay Badrinarayanan, Alex Kendall, and Roberto Cipolla. 2017. Segnet: A deep convolutional encoder-decoder architecture for image segmentation. *IEEE transactions on pattern analysis and machine intelligence*, 39(12):2481–2495.

Joost Bastings, Ivan Titov, Wilker Aziz, Diego Marcheggiani, and Khalil Sima'an. 2017. Graph convolutional encoders for syntax-aware neural machine translation. *arXiv preprint arXiv:1704.04675*.

Haochen Chen, Bryan Perozzi, Yifan Hu, and Steven Skiena. 2018a. Harp: Hierarchical representation learning for networks. In *AAAI*.

Liang-Chieh Chen, Yukun Zhu, George Papandreou, Florian Schroff, and Hartwig Adam. 2018b. Encoder-decoder with atrous separable convolution for semantic image segmentation. In *Proceedings of the European conference on computer vision (ECCV)*, pages 801–818.

Billy Chiu, Gamal Crichton, Anna Korhonen, and Sampo Pyysalo. 2016. How to train good word embeddings for biomedical nlp. In *Proceedings of the 15th workshop on biomedical natural language processing*, pages 166–174.

Fenia Christopoulou, Makoto Miwa, and Sophia Ananiadou. 2019. [Connecting the dots: Document-level neural relation extraction with edge-oriented graphs](#). In *Proceedings of the 2019 Conference on Empirical Methods in Natural Language Processing and the 9th International Joint Conference on Natural Language Processing (EMNLP-IJCNLP)*, pages 4925–4936, Hong Kong, China. Association for Computational Linguistics.

Allan Peter Davis, Cynthia J Grondin, Robin J Johnson, Daniela Sciaky, Roy McMorran, Jolene Wiegers, Thomas C Wiegers, and Carolyn J Mattingly. 2019. The comparative toxicogenomics database: update 2019. *Nucleic acids research*, 47(D1):D948–D954.

Marie-Catherine De Marneffe, Timothy Dozat, Natalia Silveira, Katri Haverinen, Filip Ginter, Joakim Nivre, and Christopher D Manning. Universal stanford dependencies: A cross-linguistic typology.

David K Duvenaud, Dougal Maclaurin, Jorge Iparraguirre, Rafael Bombarell, Timothy Hirzel, Alán Aspuru-Guzik, and Ryan P Adams. Convolutional networks on graphs for learning molecular fingerprints. In *NeurIPS*.

Hongyang Gao, Yongjun Chen, and Shuiwang Ji. 2019. Learning graph pooling and hybrid convolutional operations for text representations. In *The World Wide Web Conference*, pages 2743–2749.

Hongyang Gao and Shuiwang Ji. 2019. Graph u-nets. *arXiv preprint arXiv:1905.05178*.

Jinghang Gu, Fuqing Sun, Longhua Qian, and Guodong Zhou. 2017. Chemical-induced disease relation extraction via convolutional neural network. *Database*, 2017.

Zhijiang Guo, Yan Zhang, and Wei Lu. 2019. Attention guided graph convolutional networks for relation extraction. *ACL*.

Pankaj Gupta, Subburam Rajaram, Hinrich Schütze, and Thomas Runkler. 2019. Neural relation extraction within and across sentence boundaries. In *Proceedings of the AAAI Conference on Artificial Intelligence*, volume 33, pages 6513–6520.

Kaiming He, Xiangyu Zhang, Shaoqing Ren, and Jian Sun. 2016. Deep residual learning for image recognition. In *CVPR*, pages 770–778.

Robin Jia, Cliff Wong, and Hoifung Poon. 2019. Document-level n-ary relation extraction with multiscale representation learning. *arXiv preprint arXiv:1904.02347*.

Thomas N Kipf and Max Welling. 2016. Semi-supervised classification with graph convolutional networks. *ICLR*.

Junhyun Lee, Inyeop Lee, and Jaewoo Kang. 2019. Self-attention graph pooling. *arXiv preprint arXiv:1904.08082*.

Jiao Li, Yueping Sun, Robin J Johnson, Daniela Sciaky, Chih-Hsuan Wei, Robert Leaman, Allan Peter Davis, Carolyn J Mattingly, Thomas C Wiegers, and Zhiyong Lu. 2016a. Biocreative v cdr task corpus: a resource for chemical disease relation extraction. *Database*, 2016.

Zhiheng Li, Zhihao Yang, Hongfei Lin, Jian Wang, Yingyi Gui, Yin Zhang, and Lei Wang. 2016b. Cidextractor: A chemical-induced disease relation extraction system for biomedical literature. In *2016 IEEE International Conference on Bioinformatics and Biomedicine (BIBM)*, pages 994–1001. IEEE.

Jiongqian Liang, Saket Gurukar, and Srinivasan Parthasarathy. 2018. Mile: A multi-level framework for scalable graph embedding. *arXiv preprint arXiv:1802.09612*.

Wenjie Luo, Yujia Li, Raquel Urtasun, and Richard Zemel. 2016. Understanding the effective receptive field in deep convolutional neural networks. In *Advances in neural information processing systems*, pages 4898–4906.

Christopher D. Manning, Mihai Surdeanu, John Bauer, Jenny Finkel, Steven J. Bethard, and David McClosky. 2014. *The Stanford CoreNLP natural language processing toolkit*. In *Association for Computational Linguistics (ACL) System Demonstrations*, pages 55–60.

Diego Marcheggiani and Ivan Titov. 2017. Encoding sentences with graph convolutional networks for semantic role labeling. *EMNLP*.

Mike Mintz, Steven Bills, Rion Snow, and Dan Jurafsky. 2009. Distant supervision for relation extraction without labeled data. pages 1003–1011. *ACL*.

Makoto Miwa and Mohit Bansal. 2016. End-to-end relation extraction using lstms on sequences and tree structures. *arXiv preprint arXiv:1601.00770*.

Dat Quoc Nguyen and Karin Verspoor. 2018. Convolutional neural networks for chemical-disease relation extraction are improved with character-based word embeddings. *arXiv preprint arXiv:1805.10586*.

Thien Huu Nguyen and Ralph Grishman. 2018. Graph convolutional networks with argument-aware pooling for event detection. In *Thirty-second AAAI conference on artificial intelligence*.

Adam Paszke, Sam Gross, Francisco Massa, Adam Lerer, James Bradbury, Gregory Chanan, Trevor Killeen, Zeming Lin, Natalia Gimelshein, Luca Antiga, Alban Desmaison, Andreas Kopf, Edward Yang, Zachary DeVito, Martin Raison, Alykhan Tejani, Sasank Chilamkurthy, Benoit Steiner, Lu Fang, Junjie Bai, and Soumith Chintala. 2019. Pytorch: An imperative style, high-performance deep learning library. In *Advances in Neural Information Processing Systems 32*, pages 8024–8035.

Nanyun Peng, Hoifung Poon, Chris Quirk, Kristina Toutanova, and Wen-tau Yih. 2017. Cross-sentence n-ary relation extraction with graph lstms. *Transactions of the Association for Computational Linguistics*.

Yifan Peng, Chih-Hsuan Wei, and Zhiyong Lu. 2016. Improving chemical disease relation extraction with rich features and weakly labeled data. *Journal of cheminformatics*, 8(1):53.

Jeffrey Pennington, Richard Socher, and Christopher Manning. 2014. Glove: Global vectors for word representation. In *Proceedings of the 2014 conference on empirical methods in natural language processing (EMNLP)*, pages 1532–1543.

Chris Quirk and Hoifung Poon. 2016. Distant supervision for relation extraction beyond the sentence boundary. *EACL*.

Olaf Ronneberger, Philipp Fischer, and Thomas Brox. 2015. U-net: Convolutional networks for biomedical image segmentation. In *International Conference on Medical image computing and computer-assisted intervention*, pages 234–241. Springer.

Sunil Kumar Sahu, Fenia Christopoulou, Makoto Miwa, and Sophia Ananiadou. 2019. *Inter-sentence relation extraction with document-level graph convolutional neural network*. In *Proceedings of the 57th Annual Meeting of the Association for Computational Linguistics*, pages 4309–4316, Florence, Italy. Association for Computational Linguistics.

Linfeng Song, Yue Zhang, Zhiguo Wang, and Daniel Gildea. 2018. N-ary relation extraction using graph state lstm. *EMNLP*.

Yoshimasa Tsuruoka, Yuka Tateishi, Jin-Dong Kim, Tomoko Ohta, John McNaught, Sophia Ananiadou, and Jun’ichi Tsujii. 2005. Developing a robust part-of-speech tagger for biomedical text. In *Panhellenic Conference on Informatics*, pages 382–392. Springer.

Patrick Verga, Emma Strubell, and Andrew McCallum. 2018. *Simultaneously self-attending to all mentions for full-abstract biological relation extraction*. In *Proceedings of the 2018 Conference of the North American Chapter of the Association for Computational Linguistics: Human Language Technologies, Volume 1 (Long Papers)*, pages 872–884, New Orleans, Louisiana. Association for Computational Linguistics.

Zhitao Ying, Jiaxuan You, Christopher Morris, Xiang Ren, Will Hamilton, and Jure Leskovec. 2018. Hierarchical graph representation learning with differentiable pooling. In *NeurIPS*.

Bing Yu, Haoteng Yin, and Zhanxing Zhu. 2019. St-unet: A spatio-temporal u-network for graph-structured time series modeling. *arXiv preprint arXiv:1903.05631*.

Yuhao Zhang, Peng Qi, and Christopher D Manning. 2018. Graph convolution over pruned dependency trees improves relation extraction. *EMNLP*.

A Dataset Details

A.1 n -ary dataset

The statistics of the n -ary dataset is presented in Table 4 and Table 5. Most of the instances contain multiple sentences. Data is categorized with 5 classes: “resistance or non-response”, “sensitivity”, “response”, “resistance”, and “None”. Following prior works, the binary detection task treats all relation labels except “None” as True.

A.2 CDR dataset

We adapt our data-preprocessing from the source released by Christopoulou et al. (2019)¹⁶. The statistics is presented in Table 6. We follow (Gu et al., 2017), (Verga et al., 2018) and (Christopoulou et al., 2019) to ignore non-related pairs that correspond to general concepts (MeSH vocabulary hypernym filtering). More details can refer to (Gu et al., 2017).

B Implementation Details

Our models are developed using PyTorch (Paszke et al., 2019) and SGD optimizer is used for training. Dataset-specific implementation details are provided as follows.

B.1 n -ary dataset

B.1.1 Model architecture

The word vector is initialized by 300 dimensional GloVe embeddings (Pennington et al., 2014). We further concatenate it with 30-dimensional POS tag embedding before feeding into the Bi-LSTM

¹⁶<https://github.com/fenchri/edge-oriented-graph>

| Folds | Binary | Ternary |
|--------|--------|---------|
| fold#0 | 1256 | 1474 |
| fold#1 | 1180 | 1432 |
| fold#2 | 1234 | 1252 |
| fold#3 | 1206 | 1531 |
| fold#4 | 1211 | 1298 |

Table 4: The detailed distribution of data instances over the 5-fold on the n -ary dataset. The data partitioning is provided together with the released dataset.

| Data | Avg. Token | Avg. Sent. | Cross |
|---------|------------|------------|-------|
| Ternary | 73.0 | 2.0 | 70.1% |
| Binary | 61.0 | 1.8 | 55.2% |

Table 5: The n -ary dataset statistics. Avg. Token and Avg. Sent. are the average number of tokens and average sentence length per instance. Cross means the percentage of instance that contains multiple sentences.

| | Train | Dev | Test |
|---------------------|-------|------|------|
| Documents | 500 | 500 | 500 |
| Positive pairs | 1038 | 1012 | 1066 |
| Intra | 754 | 766 | 747 |
| Inter | 284 | 246 | 319 |
| Negative pairs | 4202 | 4075 | 4138 |
| Entities | | | |
| Chemical | 1467 | 1507 | 1434 |
| Disease | 1965 | 1864 | 1988 |
| Mentions | | | |
| Chemical | 5162 | 5307 | 5370 |
| Disease | 4252 | 4328 | 4430 |
| Avg sent. len./doc. | 25.6 | 25.4 | 25.7 |
| Avg sents./doc. | 9.2 | 9.3 | 9.7 |

Table 6: CDR dataset statistics

| | |
|------------------|------------------------------|
| Attention head | 4, 8, 10, 20 , 25 |
| Batch size | 4, 8 , 12, 16, 24, 32 |
| Sublayer (S) | 2 3 4 |
| Level (L) | 2 3 4 |

Table 7: The searching space for hyper-parameters for n -ary dataset. The bold means the best head number for multi-head self-attention and the batch size. The sublayer (S) and level (L) are different for each task in the n -ary dataset.

layer. All these vectors will be updated during training. We use one layer Bi-LSTM with 330 hidden dimensions and each GCN layer contains 200 hidden nodes. Dropout layers are used to prevent overfitting and are set to 0.5.

B.1.2 Hyper-parameters

The learning rate of SGD optimizer is initialized at 0.1 with 0.95 decay after 15 epochs. All the models are train with 200 epochs with early stopping (20 epoch). It typically stops in less than 100 epochs.

We get the attention head number of MrGCN and the training batch size based on the development set performance of MrGCN(HM) on Ternary Detection sub-task. We end up by selecting 20 heads and setting batch size equals to 8. Then, we tune our main hyper-parameter – the number of GCN layers in GCN block (S in the main context, Sublayer in Table 7) and the number of pooling times (L in the main article, Level in Table 7) for each different tasks. The hyper-parameter searching space and the best hyper-parameters for each model are listed in Table 7 and Table 8, respectively.

B.2 CDR dataset

B.2.1 Model architecture

We follow Christopoulou et al. (2019) to use the PubMed pre-trained word embedding and fix it dur-

| | Detection | | Classification | |
|---------------|-----------|--------|----------------|--------|
| | Ternary | Binary | Ternary | Binary |
| MrGCN(CM) | L4S4 | L3S2 | L2S5 | L2S4 |
| MrGCN(HM) | L3S3 | L2S2 | L3S4 | L2S2 |
| -Pool | 20 | 14 | 15 | 15 |
| MrGCN(CM)-RNN | L3S2 | L3S3 | L3S2 | L3S2 |
| MrGCN(HM)-RNN | L4S2 | L4S2 | L4S2 | L4S2 |
| -Pool-RNN | 10 | 14 | 10 | 6 |
| -Pool-Att. | 10 | 15 | 12 | 6 |

Table 8: The best Sublayer (S) and Level (L) for models in our main result and ablation studies for n -ary dataset. The total number of GCN layers can be calculated by $(2L - 1) \times S$. For models without graph pooling, we list the total number of GCN layers we use.

| | Layers | Epoch | Dev F1 |
|---------------|--------|-------|--------|
| MrGCN(CM) | L4S4 | 74 | 66.9 |
| MrGCN(HM) | L3S4 | 55 | 66.0 |
| -Pool | 12 | 41 | 65.2 |
| MrGCN(CM)-RNN | L3S3 | 72 | 64.6 |
| MrGCN(HM)-RNN | L4S4 | 58 | 64.6 |
| -RNN-Pool | 6 | 97 | 63.9 |

Table 9: The best Sublayer (S) and Level (L) for each model in our main result and ablation studies on the development set in CDR dataset. The total number of GCN layers can be calculated by $(2L - 1) \times S$. For models without graph pooling, we list the total number of GCN layers we use. We also report the epoch when each of our models gets its optimal development set performance.

ing training. The Bi-LSTM input will be the concatenation of word embedding and trainable POS-tag representations. The setup of the Bi-LSTM layers, GCN layers, and dropout layer are the same as the setting in the n -ary dataset, except that we use two layers of Bi-LSTM rather than one.

B.2.2 Hyper-parameters

The learning rate of the SGD optimizer for CDR dataset is set as 0.1 initially, and the learning rate will be decayed with scale 0.95 after 10 epochs. All the models are set to train with 200 epochs with the early stopping strategy, in which the patience is set as 15, but most of them stop within 80 epochs in the real case. We first decide the batch number by evaluating the performance on the development set, and get the best performance when the batch number is set with 16. We then train each ablation study model using the official training set and tune the sub-layer(S) and level(L) by the performance on the official development set. We use grid search to tune the sublayer from 3,4,5 and level from 2,3,4 if the experiment is with pooling mechanism. The best hyper-parameter is presented in Table 9.

$$\begin{aligned}
 A^0 &= \begin{bmatrix} n_0 & n_1 & n_2 & n_3 & n_4 & n_5 & n_6 & n_7 \\ 0 & 1 & 0 & 0 & 0 & 0 & 0 & 0 \\ 1 & 0 & 1 & 0 & 1 & 0 & 0 & 0 \\ 0 & 1 & 0 & 0 & 0 & 0 & 0 & 0 \\ 0 & 0 & 0 & 0 & 1 & 0 & 0 & 0 \\ 0 & 1 & 0 & 1 & 0 & 1 & 0 & 0 \\ 0 & 0 & 0 & 0 & 1 & 0 & 1 & 1 \\ 0 & 0 & 0 & 0 & 0 & 1 & 0 & 1 \\ 0 & 0 & 0 & 0 & 0 & 1 & 1 & 0 \end{bmatrix} & M_{0,1} &= \begin{bmatrix} m_0 & n_1 & m_1 & n_5 & m_2 \\ 1 & 0 & 0 & 0 & 0 \\ 0 & 1 & 0 & 0 & 0 \\ 1 & 0 & 0 & 0 & 0 \\ 0 & 0 & 1 & 0 & 0 \\ 0 & 0 & 1 & 0 & 0 \\ 0 & 0 & 0 & 1 & 0 \\ 0 & 0 & 0 & 0 & 1 \\ 0 & 0 & 0 & 0 & 1 \end{bmatrix} \\
 A^1 &= M_{0,1}^T A^0 M_{0,1} = \begin{bmatrix} 0 & 2 & 0 & 0 & 0 \\ 2 & 0 & 1 & 0 & 0 \\ 0 & 1 & 2 & 1 & 0 \\ 0 & 0 & 1 & 0 & 2 \\ 0 & 0 & 0 & 2 & 2 \end{bmatrix}
 \end{aligned}$$

Figure 6: The matching matrix example.

C Matching Matrices

In this section, we attach the corresponding matching matrices and illustrate how adjacency matrix A^1 can be derived from A^0 in Fig. 6, given the Hybrid Matching (HM) example in Fig. 3.

D Visualization of Clause Matching

In this section, we demonstrate a real example from the n -ary dataset to illustrate how Clause Matching (CM) works. Fig. 7a shows the original input graph in the sentence “*Preclinical data have demonstrated that afatinib is a potent irreversible inhibitor of EGFR/HER1/ErbB1 receptors including the T790M variant*.”. In order to better visualize the CM process, we omit adjacency edges in this figure.

In Fig. 7a, we can observe that nodes such as “*of*”, “*including*”, and “*.*” are disconnected from others because several dependency arcs are dropped in the original n -ary dataset, as we stated in Sec. 4.1. We show the pooled graph in Fig. 7b using CM algorithm given the input graph in Fig. 7a. If a child node is merged with its parent forming a supernode, we use the parent node to visualize the supernode. For example, “*Preclinical*” is merged with “*data*”, so we only show “*data*” in Fig. 7b.

After CM pooling, several non-core arguments of “*inhibitor*” are merged, but we can still identify the main subject of “*inhibitor*”, i.e “*afatinib*”, in the graph, which demonstrates CM’s ability on keeping the main component of a clause. The result of using CM pooling twice is shown in Fig. 7c. As depicted in the figure, although we have pooled the graph twice and have largely cut the graph size, those isolated nodes are not able to be merged. This is the reason why we hypothesize that CM does not work as well as HM in some sub-tasks of the n -ary dataset.

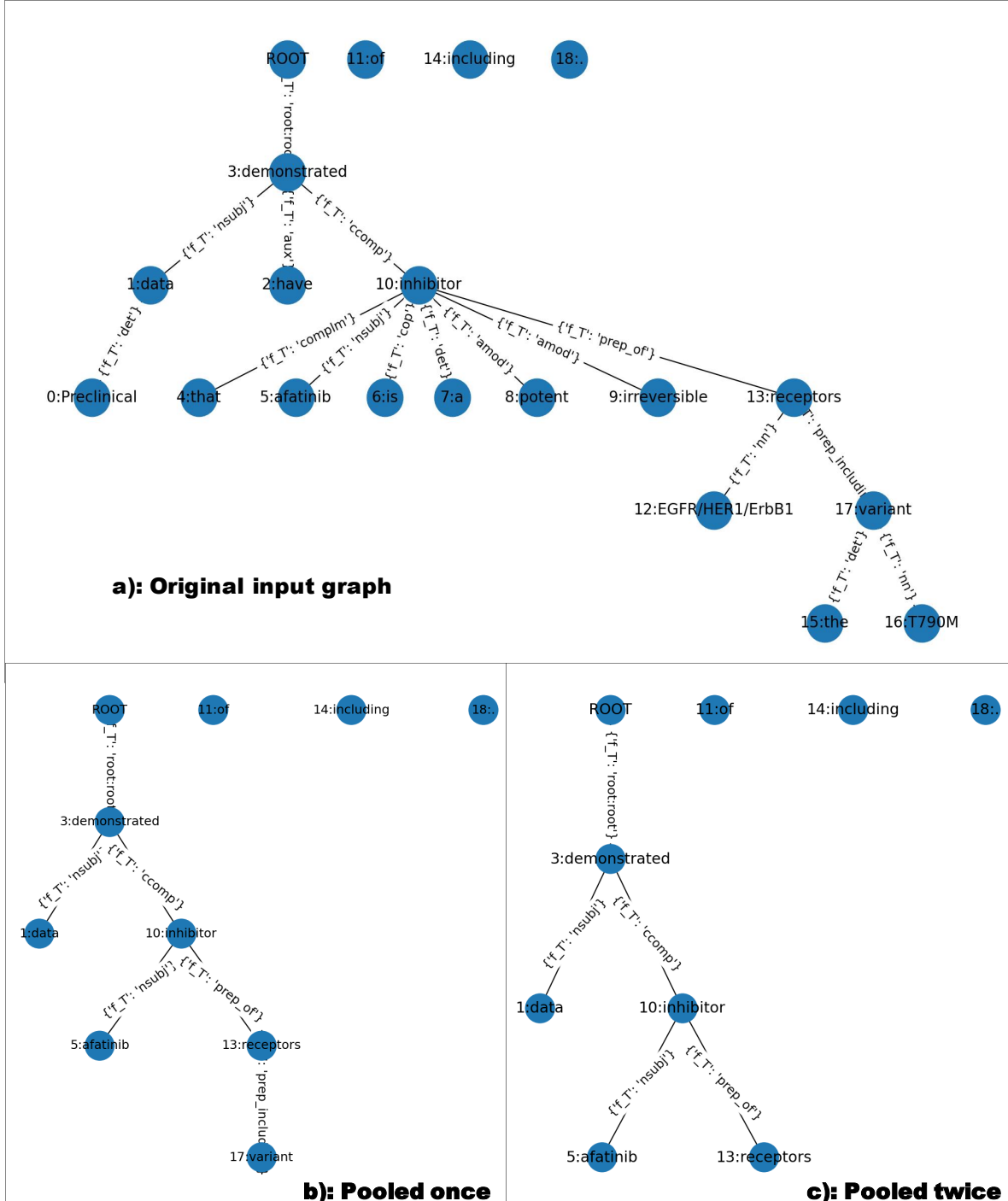


Figure 7: The visualization of Clause Matching for the input “*Preclinical data have demonstrated that afatinib is a potent irreversible inhibitor of EGFR/HER1/ErbB1 receptors including the T790M variant .*”. To better visualize the result, we omit the adjacency edges in this figure. Noted that “ROOT” does not exist in the real graph, we add the root node here in order to clearly show the tree structure.